

**Fuzzy sliding mode control for  
maximum power point tracking of a  
photovoltaic pumping system**

In this paper a new maximum power point tracking method based on fuzzy sliding mode control is proposed, and employed in a PV water pumping system based on a DC-DC boost converter, to produce maximum power from the solar panel hence more speed in the DC motor and more water quantity. This method combines two different tracking techniques sliding mode control and fuzzy logic; our controller is based on sliding mode control, then to give better stability and enhance the power production a fuzzy logic technique was added. System modeling, sliding method definition and the new control method presentation are represented in this paper. The results of the simulation that are compared to both sliding mode controller and perturbation and observation method demonstrate effectiveness and robustness of the proposed controller.

**Keywords:** Maximum power point tracking, fuzzy sliding mode control, PV water pumping system, DC-DC boost converter, fuzzy logic, sliding mode control, perturbation and observation.

Article history: Received 16 June 2016, Accepted 23 January 2017

## 1. Introduction

The worldwide demand of renewable energy has been increasing steadily, particularly in recent years. Among several renewable energy technologies, solar energy especially photovoltaic is the most promising source of energy since it produces a significant amount of energy, pollution-free and has the greatest potential for development.

PV system is mostly applied in remote and rural areas where no public grid is available and installation of a new transmission line and a transformer can be expensive. Water pumping which is studying in this paper is considering one of the servals applications of PV energy in rural areas.

The advantage of using solar energy for pumping the water is the need for large quantities of water during daytime when the sun is on top of our head, and during these times, the PV panels should produce maximum energy and hence get maximum water quantity [6].

However, the output power of PV source is influenced by environmental factors, such as temperature and illumination, also the solar cell (I-V) characteristic is nonlinear. There is a unique point on the (I-V) or (P-V) curve of the solar array called MPP, where the entire PV system operates with maximum efficiency and produces its maximum output power. In a PV panel, MPP location is not known but can be located, either through calculation models, or by search algorithms.

Therefore, to maximize the water flow rate it is necessary to optimize the PV system by adding a maximum power point tracking MPPT so that the PV array maintains operating at

\* Corresponding author: Sabah MIQOI, Laboratory of Embedded Electronic Systems and Renewable Energy, University Mohammed First Oujda, Morocco, E-mail: sabah.miq@gmail.com.

<sup>1</sup> Laboratory of Embedded Electronic Systems and Renewable Energy, University Mohammed First Oujda, Morocco

its MPP [2]. Several studies have been done in this area, thus many MPPT techniques can be found [1].

In our system, a maximum power point tracking (MPPT) algorithm controls the DC-DC converter's duty ratio [3]. This technique enables the motor armature voltage of the pump to function on its maximum speed at all-time depending on the illumination and the temperature and in turn have a maximum flow rate of the pump.

In this paper, a new MPPT controller which combines two different and powerful tracking techniques in non-linear systems, is introduced: the sliding mode control (SMC) and the fuzzy logic control (FLC).

It is well known that SMC offer good robustness and transient performance. However due to the discontinuous control action, the chattering which is defined as the oscillations around the sliding surface exists and causes the steady state performance to degrade. According to the simulation, Adding the Fuzzy Logic Control to the Sliding Mode Controller reduces these oscillations and gives better results.

In this paper, a simple photovoltaic water pumping system is presented and by using a sliding mode control to the MPPT to generate the voltage reference to which the PV system should operate, then we combine SMC with the fuzzy logic to optimize the MPPT.

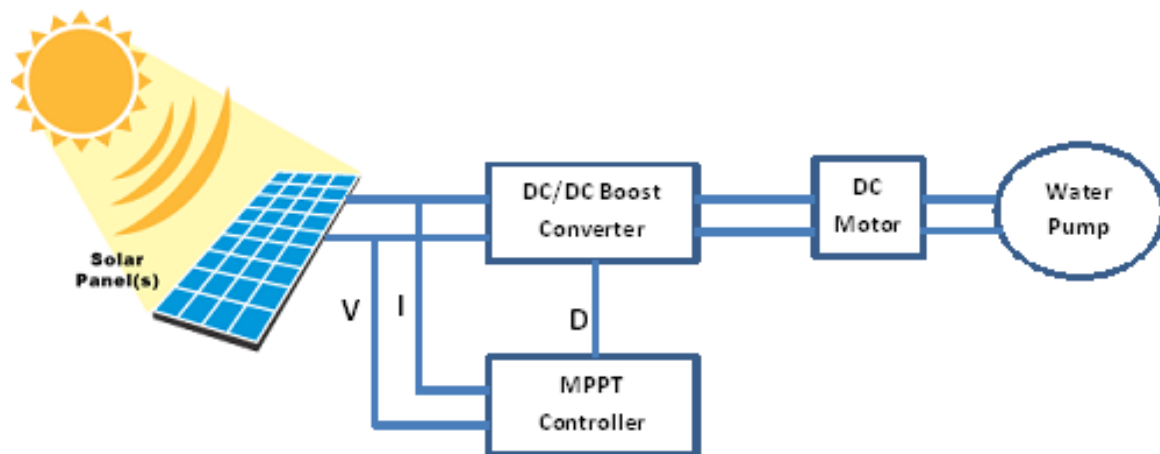


Figure 1: Proposed system

This paper is structured as follows: paragraph 2 is a description of the used PV system. Paragraph 3 introduces the concept of the sliding mode control and the fuzzy sliding mode control, applying them on our system and a brief P&O controller representation. Paragraph 4 presents the simulation results on MATLAB/Simulink of the studied system that are discussed, finally a conclusion.

## 2. System model

### 2.1. PV panel model

There are several circuit models for a PV cell but the Single-Diode model is most used because it is simpler to analyse. Figure 2 shows a Single-Diode equivalent circuit of solar cell [4].

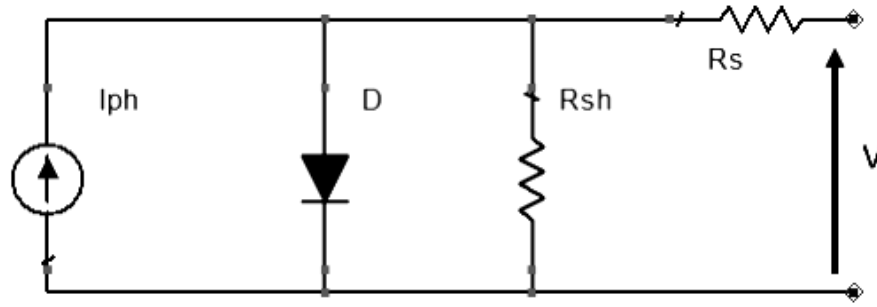


Figure 2: Circuit of solar cell

Based on Figure 2, the mathematical PV panel model is given by the equation [13]:

$$I_{pv} = N_p I_{ph} - N_p I_0 \left[ \exp \left( \frac{V_{pv} + \frac{N_s}{N_p} I_{pv} R_s}{\frac{N_s}{N_p} n V_T} \right) - 1 \right] - \frac{V_{pv} + \frac{N_s}{N_p} I_{pv} R_s}{\frac{N_s}{N_p} R_{sh}} \quad (1)$$

$N_p$  and  $N_s$  are the number of PV cells coupled in parallel and series respectively, in our case, the proposed module has an  $N_p = 1$  and  $N_s = 36$ . As result, the mathematical PV module equation becomes:

$$I_{pv} = I_{ph} - I_0 \left[ \exp \left( \frac{V_{pv} + N_s I_{pv} R_s}{N_s n V_T} \right) - 1 \right] - \frac{V_{pv} + N_s I_{pv} R_s}{N_s R_{sh}} \quad (2)$$

Where  $I_{pv}$  and  $V_{pv}$  are the current and voltage, respectively, of the PV module

$I_{ph}$  : The photovoltaic current, A

$I_0$  : Reverse saturation current, A

$R_s$  : Series resistance of the cell,  $\Omega$

$R_{sh}$  : Shunt resistance of the cell,  $\Omega$

$V_T = \frac{kT}{q}$  : Thermal voltage, V

k: Boltzmann constant ( $k = 1,38 \cdot 10^{-23}$  J/K)

q: the electron charge ( $q = 1,602 \cdot 10^{-19}$  C)

T: the module temperature, K

n: the diode ideality factor ( $n = 1.62$ ).

The characteristics of the panel for a fixed temperature and variable irradiation are represented in the figure 3:

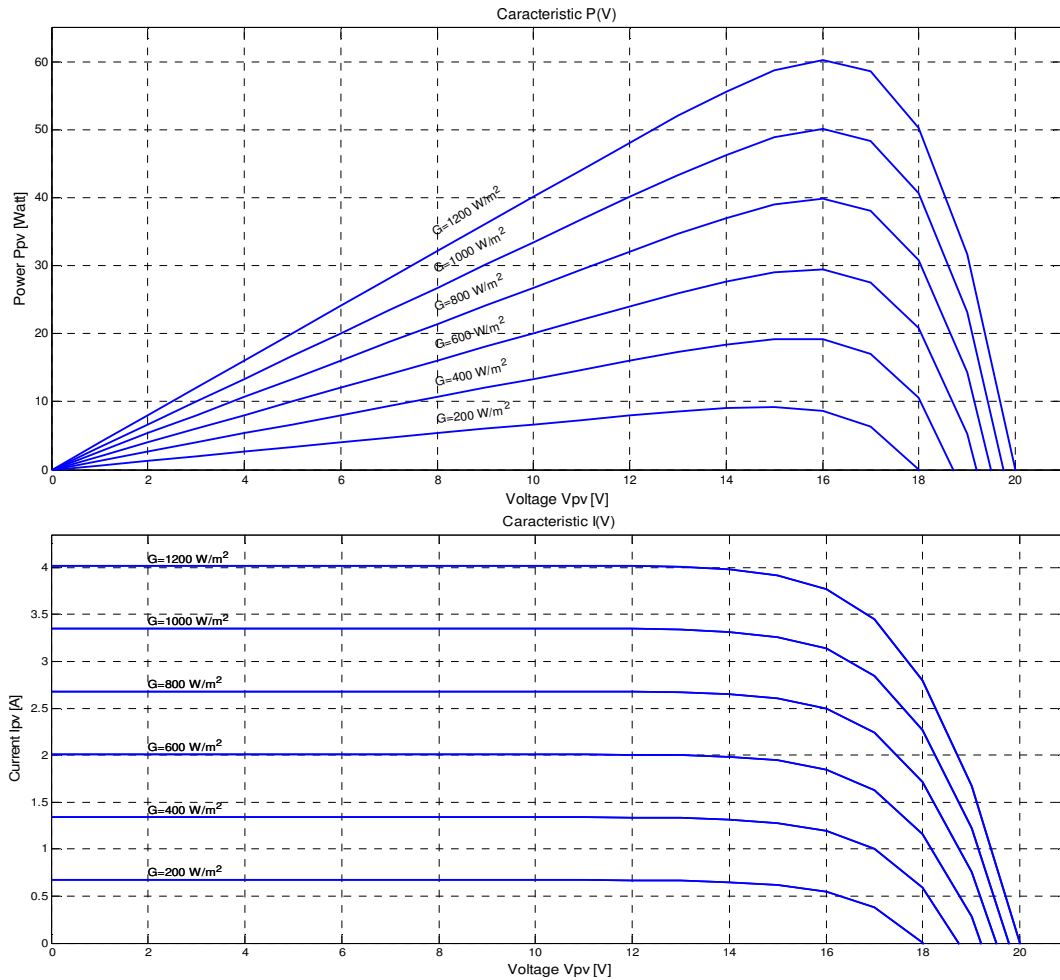


Figure 3: PV characteristics under different irradiation and temperature conditions

## 2.2. DC-DC Boost converter

The Figure 4 shows the circuit of a boost converter. This circuit is used when a higher output voltage than input is required.

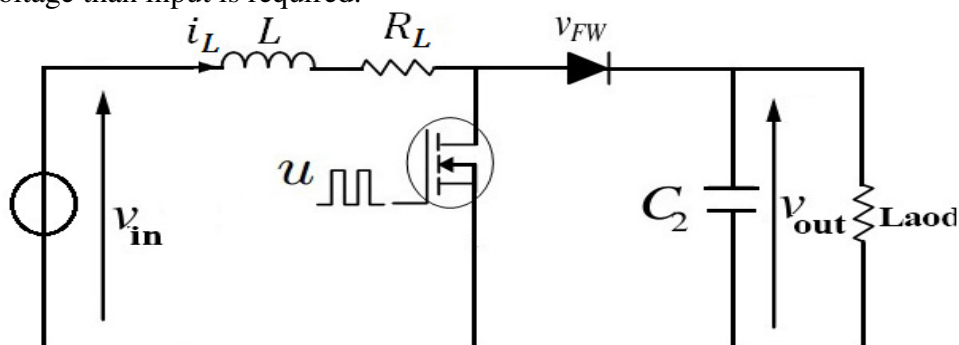


Figure 4: Boost converter

During the on state, namely the switch is closed:

$$V_{in} = L \frac{di_L}{dt} \tag{3}$$

During the off state, the switch is open:

$$V_{in} - V_{out} = L \frac{di_L}{dt} \tag{4}$$

Since the average voltage across L is zero

$$V_L = DV_{in} + (1 - D)(V_{in} + V_{out}) = 0 \quad (5)$$

The input/output equation becomes:

$$V_{out} = \frac{V_{in}}{1-D} \quad (6)$$

D represent the duty cycle.

### 2.3. DC motor

The system structure of a DC motor is represented in Figure 5, including the armature resistance  $R_a$  and inductance  $L_a$ .

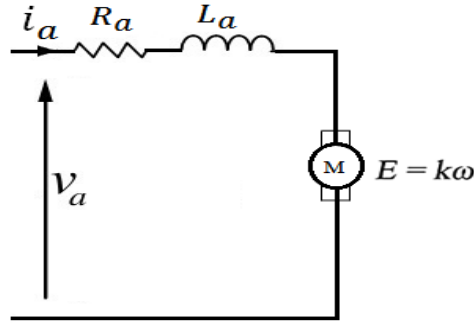


Figure 5: DC motor

The dynamic equations of the DC motor are:

$$V_a = R_a i_a + L_a \frac{di_a}{dt} + k\omega \quad (7)$$

$$j \frac{d\omega}{dt} + k_2\omega - k i_a = -k_1 \quad (8)$$

### 2.4. Centrifugal pump model

A pump is a machine that converts the input mechanical power into output fluid power. It is coupled directly to the motor and is characterized by torque, speed and flow.

We have chosen to use a centrifugal pump due to their reduced price and are available for a wide range of flow rate.

The pumps are generally described by their characteristics  $H(Q)$ .  $H$  (in meters) is the hydraulic load and  $Q$  ( $m^3 / s$ ) is the flow rate of the pump, and is described by the formula:

$$H = a\omega^2 + b\omega Q + cQ^2 \quad (9)$$

The constant  $a$ ,  $b$  and  $c$  are determined according to the manufacturer's measurement data.

The hydraulic power in Watt, is given by:

$$P_H = \rho g Q H \quad (10)$$

$\rho$  is the density ( $1000Kg/m^3$ )

### 2.5. The model of the whole system

Our photovoltaic pumping system consists of a PV panel, a DC-DC Boost converter, a DC motor and a water pump. Figure 6 shows the equivalent circuit of the boost system based on PV with water pump [7, 6].

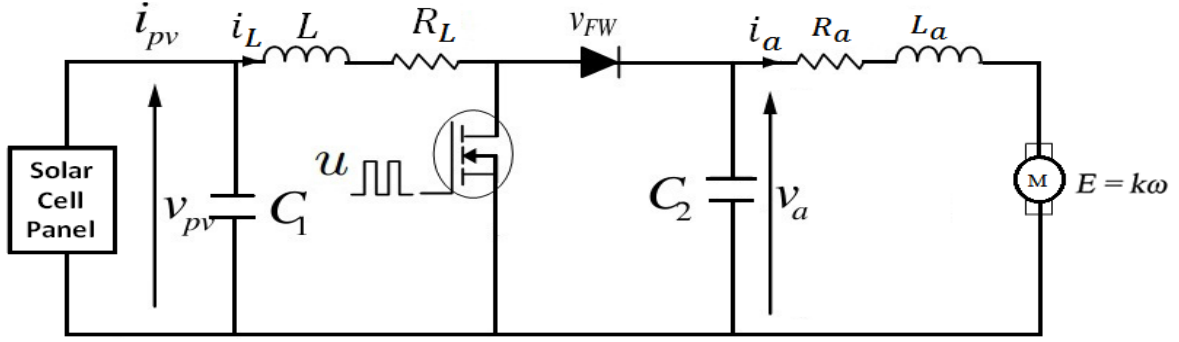


Figure 6: Equivalent circuit of the system

The system's average model is given in the equations below:

$$\left\{ \begin{aligned} \frac{di_L}{dt} &= \frac{V_{pv}}{L} - \frac{R_L}{L} i_L + \frac{-R_m i_L + V_{FW} + V_a}{L} u - \frac{V_{FW}}{L} - \frac{V_a}{L} \\ \frac{dV_{pv}}{dt} &= \frac{i_{pv}}{C_1} - \frac{i_L}{C_1} \\ \frac{di_a}{dt} &= \frac{-R_a}{L_a} i_a + \frac{V_a}{L_a} - \frac{k}{L_a} \omega \\ \frac{dV_a}{dt} &= -\frac{i_a}{C_2} + \frac{i_L}{C_2} - \frac{i_L}{C_2} u \\ \frac{d\omega}{dt} &= \frac{k}{j} i_a - \frac{k_2}{j} \omega - \frac{k_1}{j} \end{aligned} \right. \quad (11)$$

Where  $u$  is the control input.  $V_a$ ,  $i_a$ ,  $R_a$  and  $L_a$  are the motor's armature voltage, current, resistance and inductance successively.  $L$ ,  $R_L$  and  $i_L$  are the self-inductance, resistance and current.  $R_m$  is the resistance characterizing IGBT lost.  $C_1$  and  $C_2$  are the input and the output capacitance respectively.  $V_{FW}$  is the diode forward voltage.  $\omega$  is DC-motor speed.

$j$ ,  $k$ ,  $k_1$ , and  $k_2$  are respectively the moment of inertia of the motor, the motor's torque constant, the load of torque and the viscous friction coefficient

The state representation of the system is written as:

$$\frac{d}{dt} \begin{pmatrix} i_L \\ V_{pv} \\ i_a \\ V_a \\ \omega \end{pmatrix} = \begin{pmatrix} -\frac{R_L}{L} & \frac{1}{L} & 0 & -\frac{1}{L} & 0 \\ -\frac{1}{C_1} & 0 & 0 & 0 & 0 \\ 0 & 0 & -\frac{R_a}{L_a} & \frac{1}{L_a} & -\frac{k}{L_a} \\ \frac{1}{C_2} & 0 & -\frac{1}{C_2} & 0 & 0 \\ 0 & 0 & \frac{k}{j} & 0 & -\frac{k_2}{j} \end{pmatrix} \begin{pmatrix} i_L \\ V_{pv} \\ i_a \\ V_a \\ \omega \end{pmatrix} + \begin{pmatrix} \frac{-R_m i_L + V_{f\omega} + V_a}{L} \\ 0 \\ 0 \\ -\frac{i_L}{C_2} \\ 0 \end{pmatrix} u + \begin{pmatrix} -\frac{V_{f\omega}}{L} \\ \frac{i_{pv}}{C_1} \\ 0 \\ 0 \\ -\frac{k_1}{j} \end{pmatrix} \quad (12)$$

The system can be represented as:

$$\dot{x} = A \cdot x + b(x)u + d \quad (13)$$

Where the vector state is given by:

$$x = \begin{pmatrix} i_L \\ V_{pv} \\ i_a \\ V_a \\ \omega \end{pmatrix} \quad (14)$$

and

$$A = \begin{pmatrix} -\frac{R_L}{L} & \frac{1}{L} & 0 & -\frac{1}{L} & 0 \\ -\frac{1}{C_1} & 0 & 0 & 0 & 0 \\ 0 & 0 & -\frac{R_a}{L_a} & \frac{1}{L_a} & -\frac{k}{L_a} \\ \frac{1}{C_2} & 0 & -\frac{1}{C_2} & 0 & 0 \\ 0 & 0 & \frac{k}{j} & 0 & -\frac{k_2}{j} \end{pmatrix} \quad b(x) = \begin{pmatrix} -\frac{R_m i_L + V_f \omega + V_a}{L} \\ 0 \\ 0 \\ -\frac{i_L}{C_2} \\ 0 \end{pmatrix} \quad d = \begin{pmatrix} -\frac{V_f \omega}{L} \\ \frac{i_{pv}}{C_1} \\ 0 \\ 0 \\ -\frac{k_1}{j} \end{pmatrix} \quad (15)$$

### 3. MPPT control description

#### 3.1. P&O

A comparison between the two controllers SMC and FSMC, applying to the perturbation and observation method (P&O), is proposed. The choose of the P&O is due to the fact that it is the most used method to control the MPP in the industry, and for its simplicity and efficiency.

The characteristics of PV panel are measured and then induce a small perturbation on the voltage (or current) to analyse the resulting power variation [20].

Figure 7 shows the flowchart of the P&O algorithm which should be implemented.

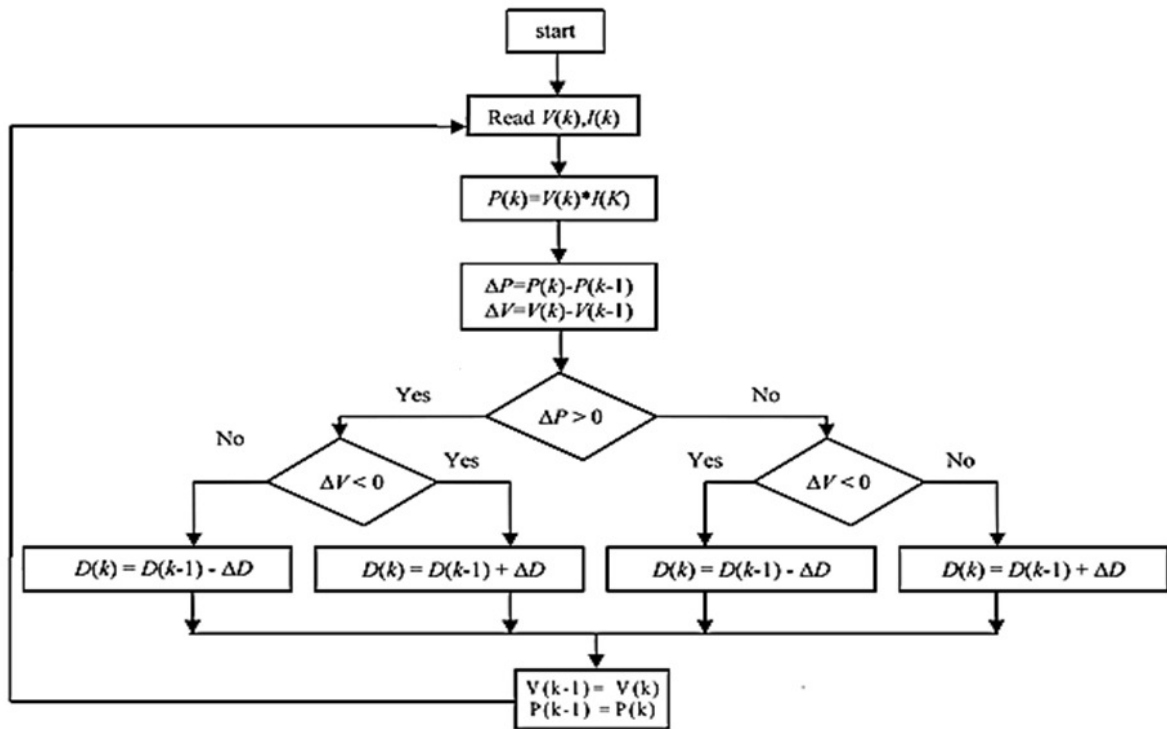


Figure 7: P&O flowchart

### 3.2. Sliding mode control

Sliding Mode Control is a nonlinear control solution and a variable structure control (VSC). It was proposed by Vladimir UTKIN in (Utkin, 1977) [14]. The advantages of SMC are various and important: high precision, good stability, simplicity, invariance, robustness...

The design of the control can be obtained in two important steps [15, 17]:

- The choice of the sliding surface:

The MPP is determined when:

$$\frac{\partial P_{pv}}{\partial V_{pv}} = 0 \tag{16}$$

Therefore, the sliding surface is defined as:

$$s = \frac{\partial P_{pv}}{\partial V_{pv}} = \frac{\partial I_{pv}^2 R_{pv}}{\partial V_{pv}} = I_{pv} + V_{pv} \frac{\partial I_{pv}}{\partial V_{pv}} = 0 \tag{17}$$

- The determination of the control law [11]:

The structure of the sliding mode control consists of two parts: the first one deal with the equivalent control quantity  $u_{eq}$ , which maintain the operation point in the switching surface and displace it to the origin, and the second one provides the stabilization of the controller  $u_n$  :

$$u = u_{eq} + u_n \tag{18}$$

The equivalent control suggested by Slotine and Li (2005) is determined from the following condition [12]:

$$\dot{s} = \left[ \frac{\partial s}{\partial x} \right]^T \dot{x} = \left[ \frac{\partial s}{\partial x} \right]^T (A \cdot x + b(x)u + d) = 0 \quad (19)$$

Considering  $d = 0$ , to simplify the calculations (which is not real), the equivalent control is [16]:

$$u_{eq} = - \frac{\left[ \frac{\partial s}{\partial x} \right]^T (A \cdot x)}{\left[ \frac{\partial s}{\partial x} \right]^T b(x)} \quad (20)$$

The stabilization part of the control  $u_n$  can be a linear function of the sliding surface  $s$ , which permits to attract the sliding surface and to soften the operating point at its optimum:  $u_n$  is given by [18]:

$$u_n = -k_s \cdot \text{sgn}(s) \quad (21)$$

$k_s$  is a positive constant which is determined by the user and  $\text{sgn}$  designates the sign function.

The range of  $k_s$  can be determined ensuring  $s\dot{s} < 0$ .

$$\text{sgn}(s) = \begin{cases} -1 & \text{if } s < 0 \\ 0 & \text{if } s = 0 \\ 1 & \text{if } s > 0 \end{cases} \quad (22)$$

Thus the SMC controller is:

$$u = - \frac{\left[ \frac{\partial s}{\partial x} \right]^T (A \cdot x)}{\left[ \frac{\partial s}{\partial x} \right]^T b(x)} - k_s \cdot \text{sgn}(s) \quad (23)$$

Stabilization study [19]:

We chose to use a function named Lyapunov given by:

$$V = \frac{1}{2} s^2 \quad (24)$$

The derivative of this function is equal zero:

$$\dot{V} = s\dot{s} < 0 \quad \forall s \neq 0 \quad (25)$$

$$s = I_{pv} + V_{pv} \frac{\partial I_{pv}}{\partial V_{pv}} = 0 \quad (26)$$

$$I_{pv} = I_{ph} - I_0 \left[ \exp \left( \frac{V_{pv} + N_S I_{pv} R_S}{N_S n V_T} \right) - 1 \right] - \frac{V_{pv} + N_S I_{pv} R_S}{N_S R_{Sh}} \quad (27)$$

$$\frac{\partial I_{pv}}{\partial V_{pv}} = - \frac{I_0}{N_S n V_T} \exp \left( \frac{V_{pv} + N_S I_{pv} R_S}{N_S n V_T} \right) - \frac{1}{N_S R_{Sh}} \quad (28)$$

$$s = I_{ph} - I_0 \left[ \exp \left( \frac{V_{pv} + N_S I_{pv} R_S}{N_S n V_T} \right) - 1 \right] - \frac{V_{pv} + N_S I_{pv} R_S}{N_S R_{Sh}} - \left[ \frac{V_{pv} I_0}{N_S n V_T} \exp \left( \frac{V_{pv} + N_S I_{pv} R_S}{N_S n V_T} \right) + \frac{V_{pv}}{N_S R_{Sh}} \right] \quad (29)$$

$$s = I_{ph} - I_0 \exp\left(\frac{V_{pv} + N_s I_{pv} R_s}{N_s n V_T}\right) \left[1 + \frac{V_{pv}}{N_s n V_T}\right] - \frac{2V_{pv} + N_s I_{pv} R_s}{N_s R_{sh}} + I_0 \quad (30)$$

The derivative is given by:

$$\dot{s} = \frac{\partial s}{\partial V_{pv}} \cdot \frac{\partial V_{pv}}{\partial t} \quad (31)$$

$$\dot{s} = - \left[ \frac{V_{pv} I_0}{N_s n V_T} \exp\left(\frac{V_{pv} + N_s I_{pv} R_s}{N_s n V_T}\right) \left[2 + \frac{V_{pv}}{N_s n V_T}\right] + \frac{2}{N_s R_{sh}} \right] \frac{\partial V_{pv}}{\partial t} \quad (32)$$

After approximation, we get:

$$\dot{s} = - \left[ 2 \frac{V_{pv} I_0}{N_s n V_T} \exp\left(\frac{V_{pv} + N_s I_{pv} R_s}{N_s n V_T}\right) \right] \frac{\partial V_{pv}}{\partial t} \quad (33)$$

When  $s > 0$ , as shown in figure 8 the system operates on the left side of the MPP, therefore the voltage must be increased to attain the MPP which means  $\frac{\partial V_{pv}}{\partial t} > 0$ , replacing in equation we would have  $\dot{s} < 0$ , and hence  $s\dot{s} < 0$ .

When  $s < 0$ , the system operates on the right side of the MPP, the voltage must be decreased to attain the MPP which means  $\frac{\partial V_{pv}}{\partial t} < 0$  and  $\dot{s} > 0$ , therefore  $s\dot{s} < 0$ .

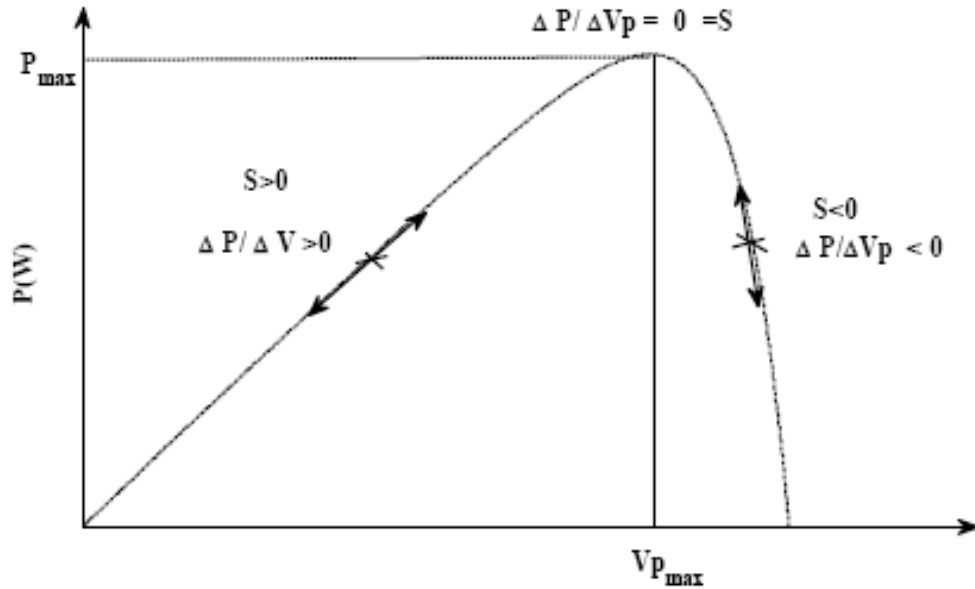


Figure 8: Operating point and the sign of the sliding surface

As a result, the system can reach stability regardless of the position of the MPP on the right or on the left.

### 3.3. Fuzzy sliding mode control

As described in the last section, the objective of the SMC is to design a control law that consists of an equivalent control and a stabilization control. In this section, we developed a fuzzy logic control to accomplish the stabilization part then to optimize the controller and reduce the chattering phenomena. The proposed control is called Fuzzy Sliding Mode Control.

The structure of the fuzzy sliding mode control is:

$$u = u_{eq} + u_f \tag{34}$$

We recall that the equivalent control is given by:

$$u_{eq} = - \frac{\left[ \frac{\partial s}{\partial x} \right]^T (A.x)}{\left[ \frac{\partial s}{\partial x} \right]^T b(x)} \tag{35}$$

The proposed FSMC is shown in figure 10, where  $s$  and  $\dot{s}$  are the inputs and  $u$  the output of the FSMC.

Fuzzy logic control consists of three stages: as we can see in figure 9: Fuzzification, inference and defuzzification [22].

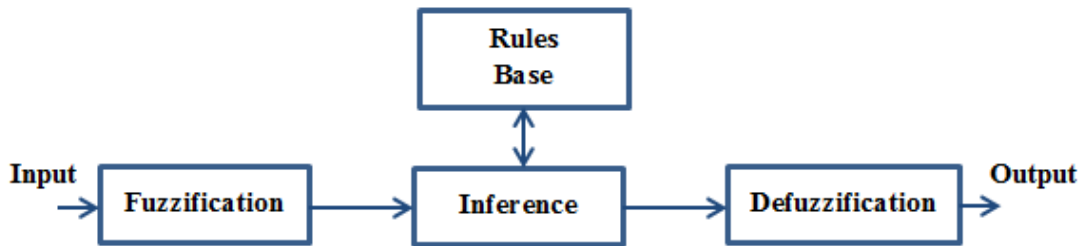


Figure 9: Fuzzy controller block diagram

- **Fuzzification:** convert numerical input variables into linguistic variables based on a membership function. In our case, three fuzzy levels are used for the tow input  $s$  and  $\dot{s}$ , which are N to (negative), Z (zero) and PS (positive), and for the output  $u_f$  five fuzzy levels are used, NB (negative big), NS (negative small), ZE (zero), PS (positive small), and PB (positive big), and we associate to each of the real inputs a degree of membership between 0 and 1 [10].

- **Inference:** it is associated with the basic types of rules: "If ... Then ..."The fuzzy inference step is carried out by Mamdani's method table shows fuzzy base rules.

- **Defuzzification:** aims to transform the fuzzy sets defined by the inference mechanism to a numerical value. The defuzzification uses the centre of gravity technique [5, 21].

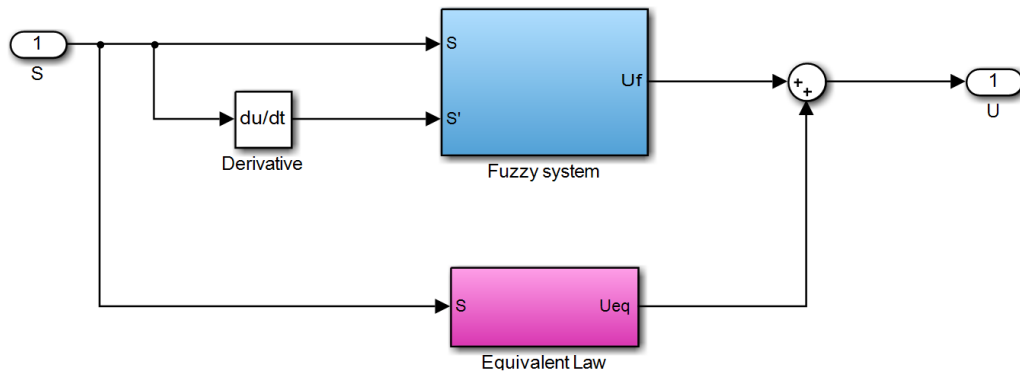


Figure 10: Insertion of fuzzy logic into the sliding mode control in Matlab

The membership functions for these fuzzy sets corresponding to  $s, s'$  and  $u_f$  are defined in figure 11:

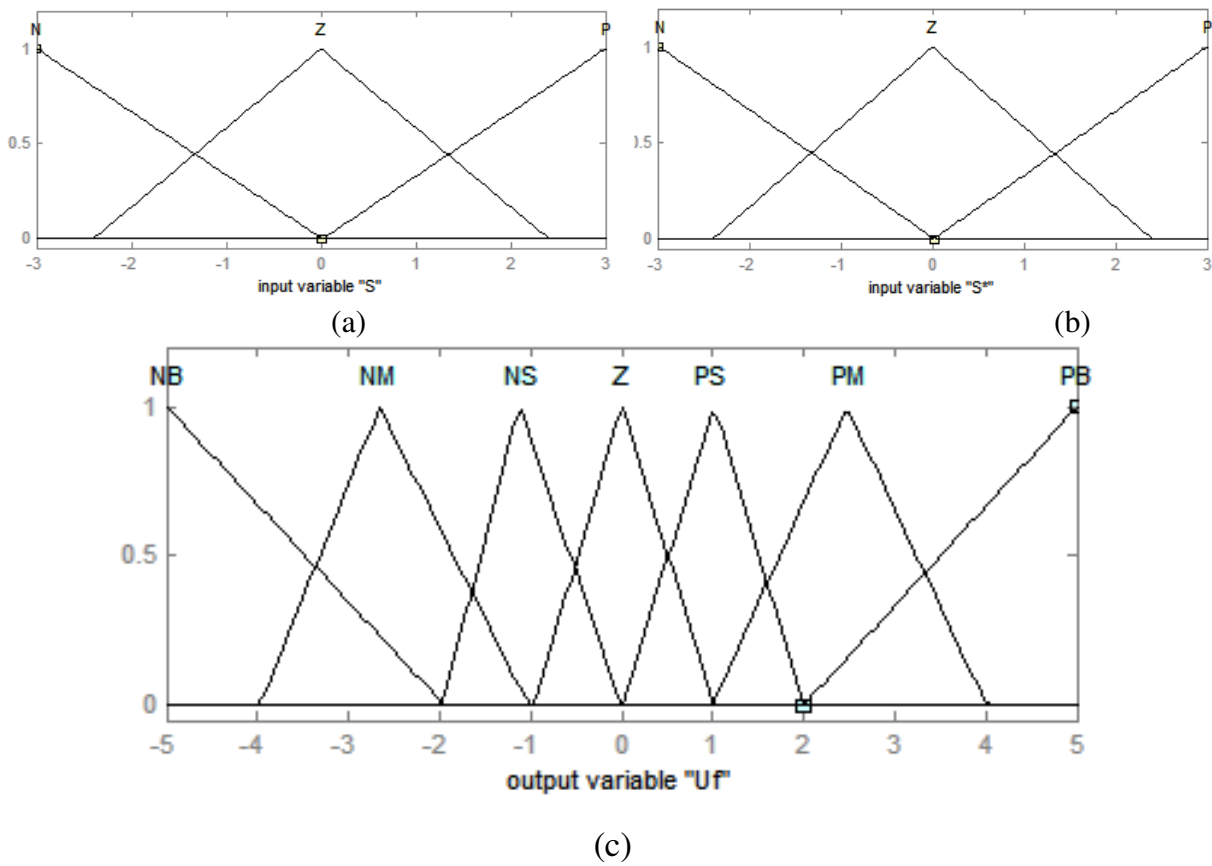


Figure 11: Membership functions (a) sliding surface (b) sliding surface derivative (c) the fuzzy control

Table 1: Rules base

| $u_f$    | $S$      |          |          |
|----------|----------|----------|----------|
|          | <b>N</b> | <b>Z</b> | <b>P</b> |
| <b>N</b> | PB       | PM       | PS       |
| <b>Z</b> | PS       | ZE       | NS       |
| <b>P</b> | NS       | NM       | NB       |

#### 4. Results

The water pumping PV system based on boost converter with the three controllers SMC, FSMC and P&O has been implemented and simulated in MATLAB/Simulink. The panel solar used in this research is TE500CR [9].

Table 2: Parameters of the system components

|                      |                               |                      |  |
|----------------------|-------------------------------|----------------------|--|
| <b>R<sub>L</sub></b> | 0.5 $\Omega$                  | <b>C<sub>1</sub></b> | 6.2 $10^{-3}$ F                            |
| <b>R<sub>a</sub></b> | 1.254 $\Omega$                | <b>L</b>             | 6.8 $10^{-3}$ H                            |
| <b>J</b>             | 0.004 kg.m <sup>2</sup>       | <b>k<sub>2</sub></b> | 0.0114 kg.m <sup>2</sup> /sec <sup>2</sup> |
| <b>C<sub>2</sub></b> | 2.88 $10^{-3}$ F              | <b>L<sub>a</sub></b> | 28 $10^{-3}$ H                             |
| <b>k<sub>1</sub></b> | 0.1kg.m <sup>2</sup> .rad/sec | <b>K</b>             | 0.333 V.sec/rad                            |

We compare the results of the panel power, the speed and the float rate of each controller used in this system.

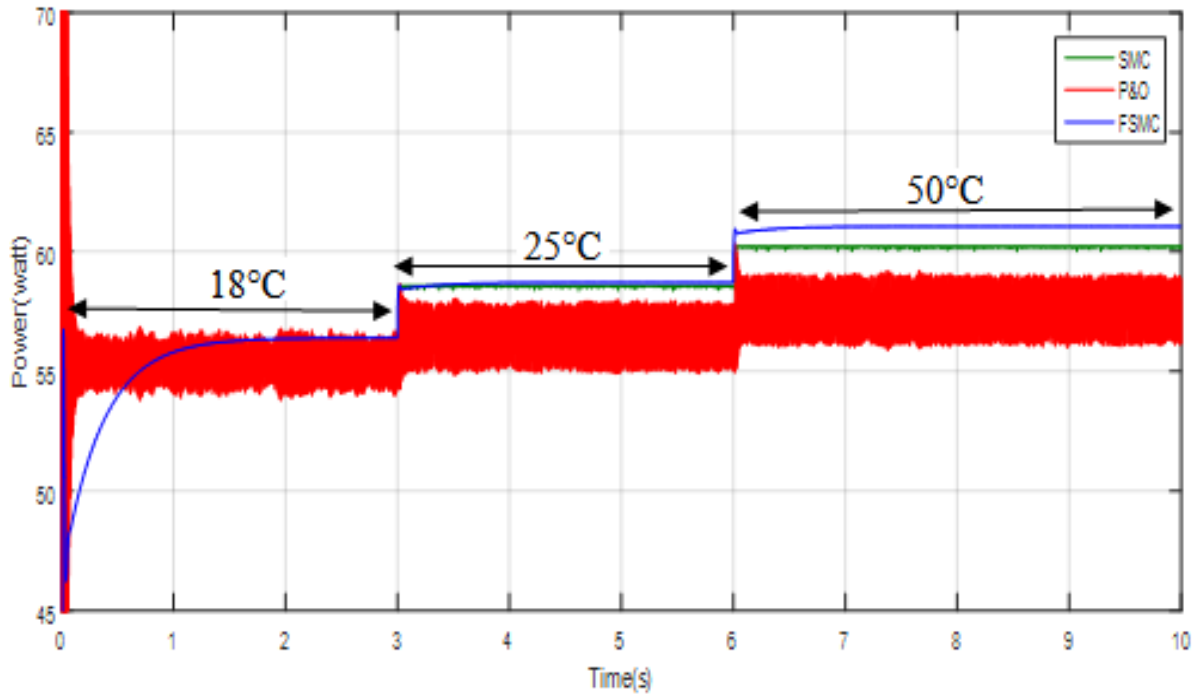


Figure 12: Comparison of SMC, FSMC and P&O power performance for different solar temperature input

Figure 12 shows the power performance of the proposed FSMC compared to SMC and P&O for constant irradiation of  $1000\text{W/m}^2$  and variable temperature from  $18^\circ\text{C}$  to  $25^\circ\text{C}$  to  $50^\circ\text{C}$ . It can be seen from figure 12 that FSMC has better performance with less oscillation compared to P&O.

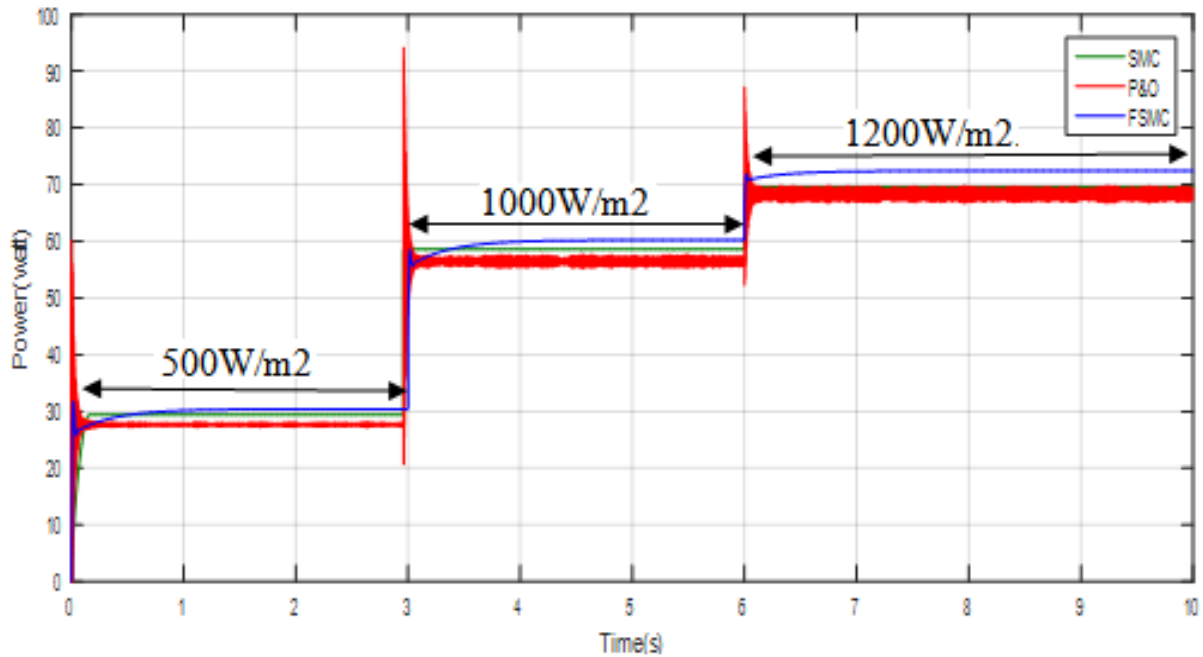


Figure 13: Comparison of SMC, FSMC and P&O power performance for different solar irradiation input

Figure 13 compares the power performance of the three controllers under constant temperature of 25°C and variable solar irradiation from 500W/m<sup>2</sup> to 1000W/m<sup>2</sup> to 1200W/m<sup>2</sup>. The fuzzy sliding mode controller demonstrates again more accurate performance.

In order to evaluate the performance of the proposed method, we calculate the efficiency of each MPPT method. Equation defines the MPPT efficiency:

$$\eta_{MPPT} = \frac{\int P_{actual}}{\int P_{max}}$$

Where  $P_{actual}$  is the produced power with the specific MPPT controller and  $P_{max}$  is the ideal or theoretical maximum power the PV array can produce under given temperature and irradiation.

Figure 14 demonstrates the effectiveness of the system for the three controllers, the temperature is maintained at 25°C and the solar irradiation changes from 600W/m<sup>2</sup> to 1000W/m<sup>2</sup> with step of 50W/m<sup>2</sup>. The controller FSMC shows higher efficiency compared to the two other controllers P&O and SMC.

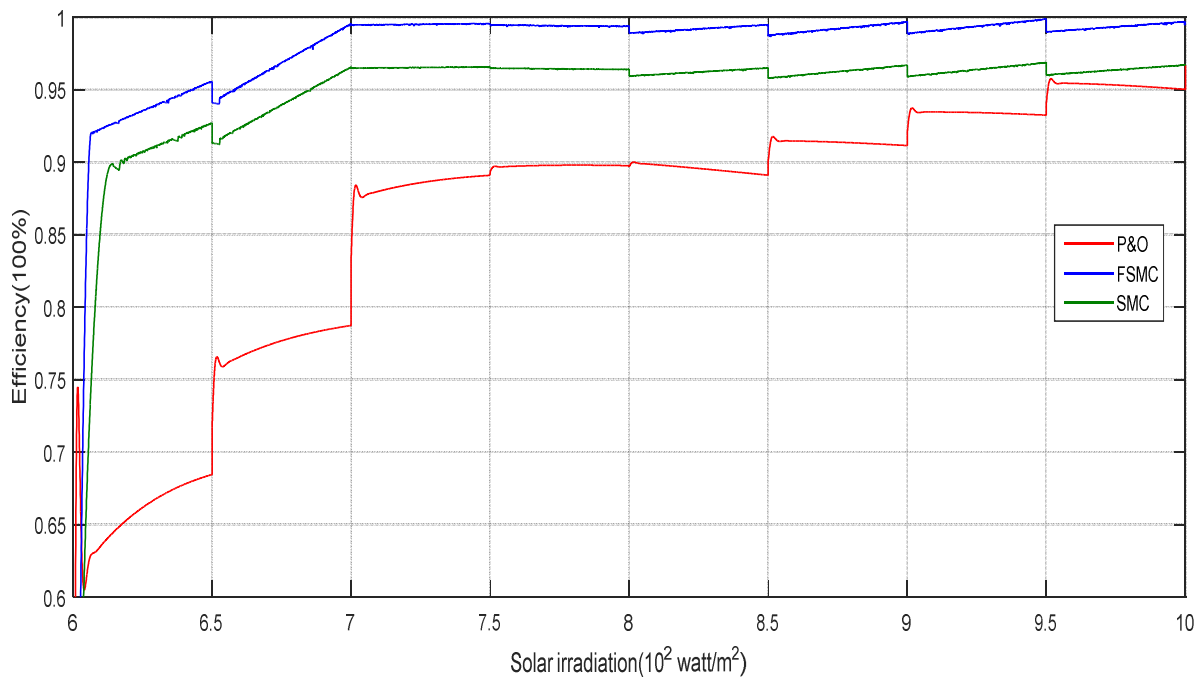


Figure 14: Efficiency of the controller for different solar irradiances

This section presents the simulation results to check the effectiveness of the proposed control via MATLAB in variable atmospheric conditions (temperature and irradiation for a whole day) [8].

Figure 15 and 16 present the climatic conditions on one day (temperature and solar irradiance).

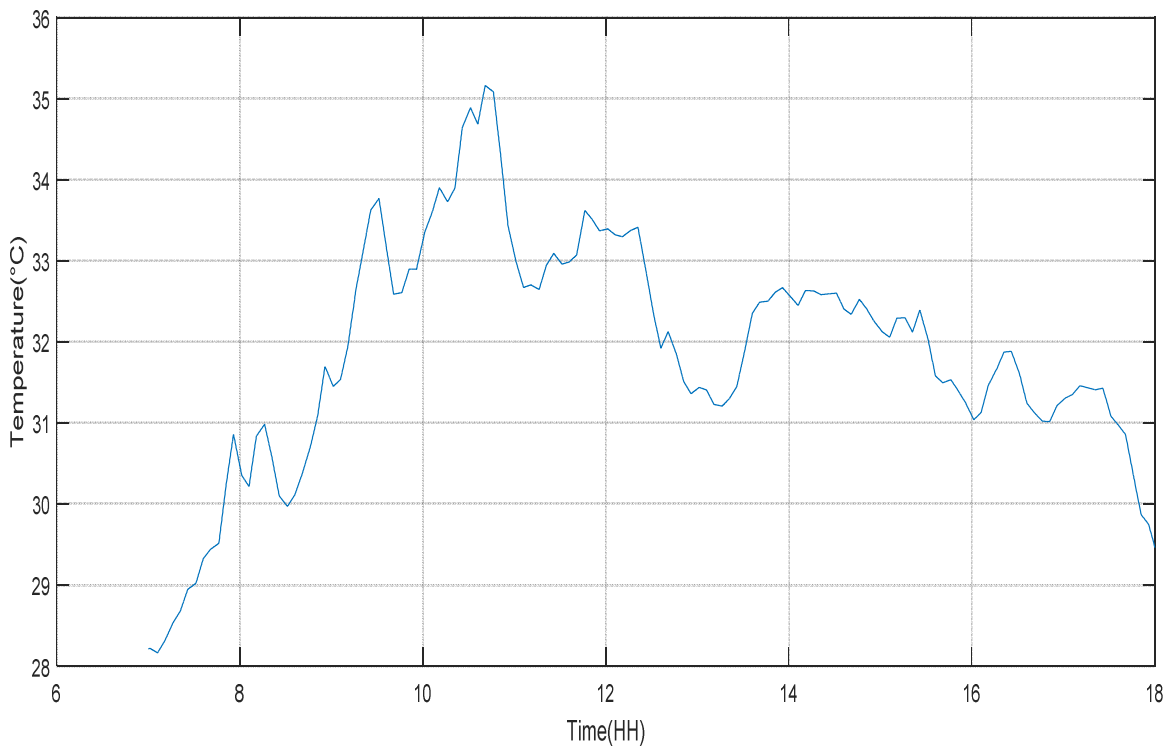


Figure 15: Cell temperature for a day

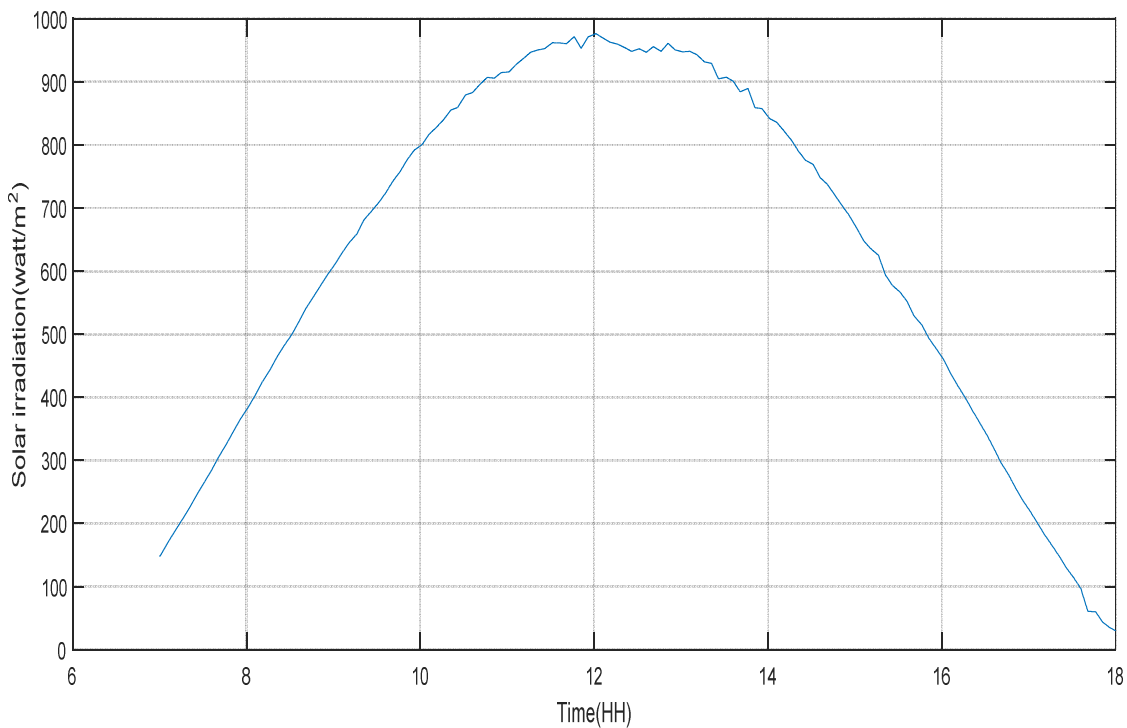


Figure 16: Solar irradiation for a day

Figure 17, 18, 19 and 20 show respectively the development of the power the motor speed, the flow rate and the motor armature voltage.

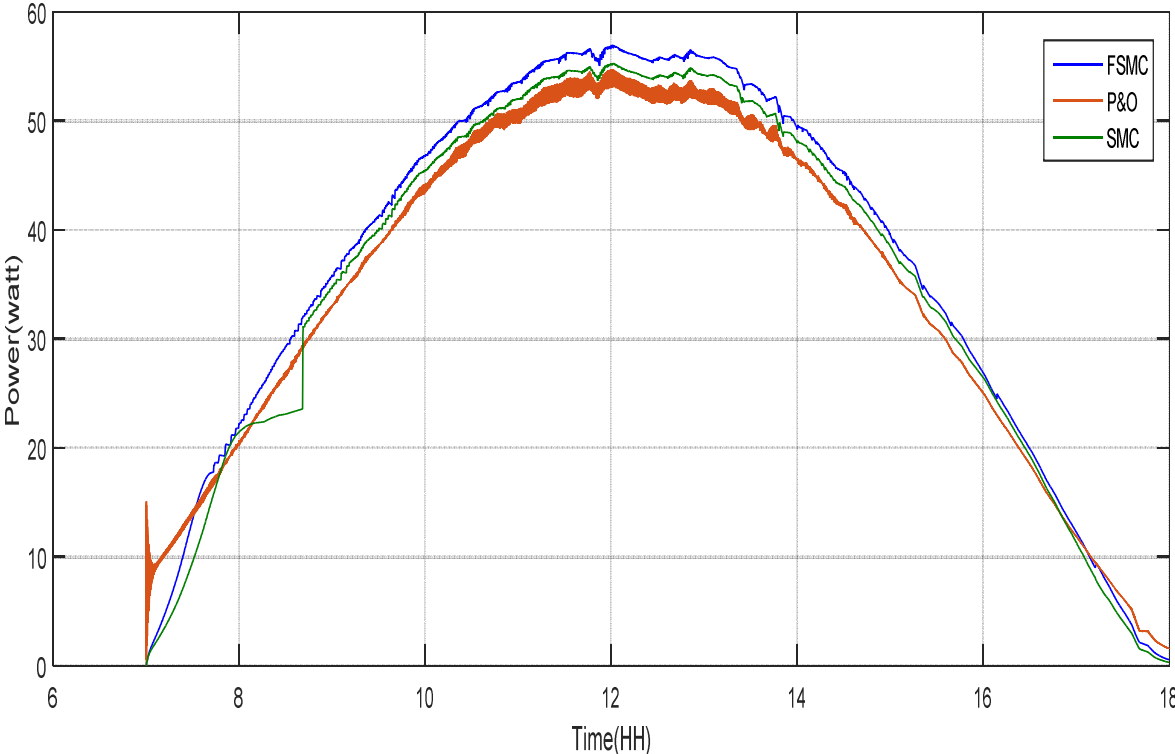


Figure 17: Comparison of the power generated by the three controllers

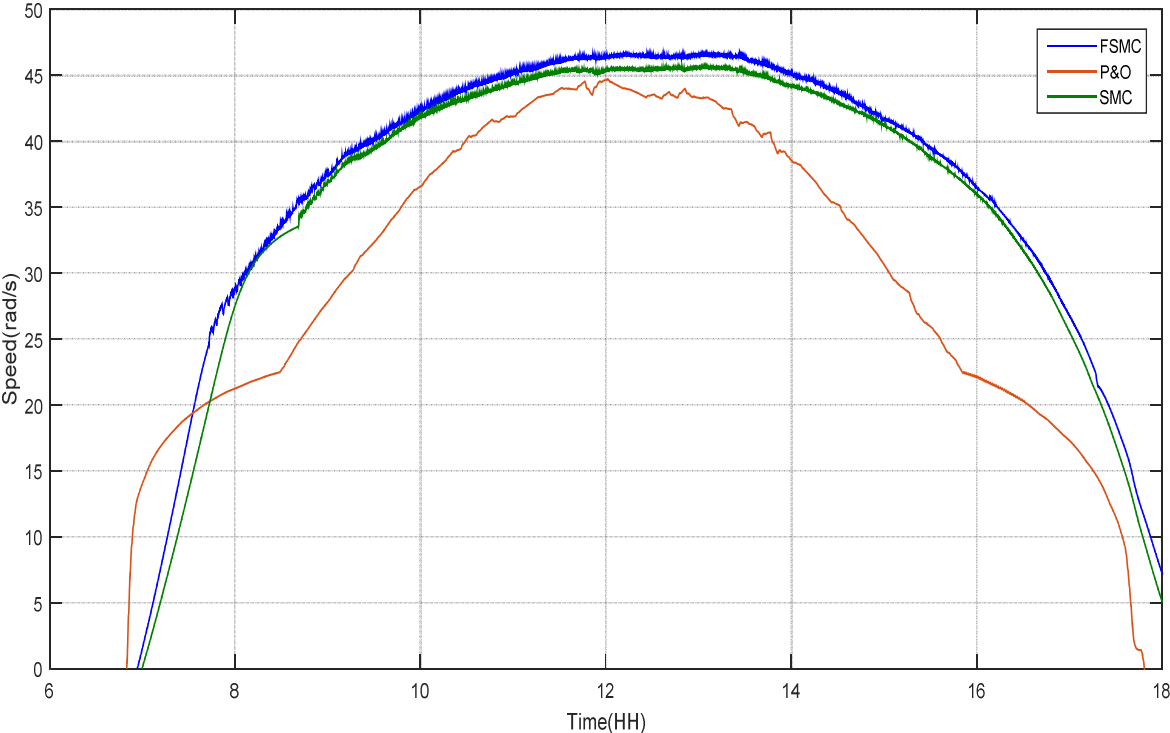


Figure 18: DC motor speed comparison for the three controller

Figures 17,18,19 and 20 demonstrate that the proposed FSMC controller shows better results than the P&O and the SMC.

The increase of the DC motor speed leads to the increase of the flow rate of the water pump.

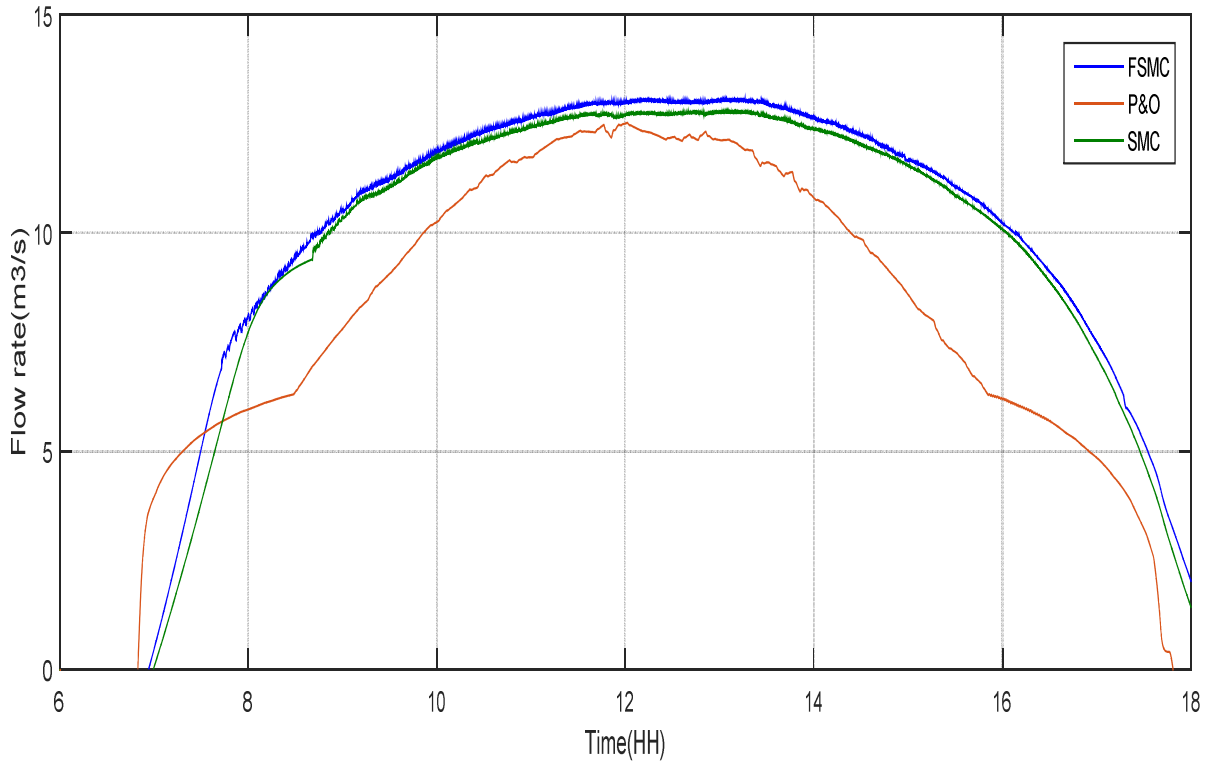


Figure 19: comparison of Flow rate of the water pump

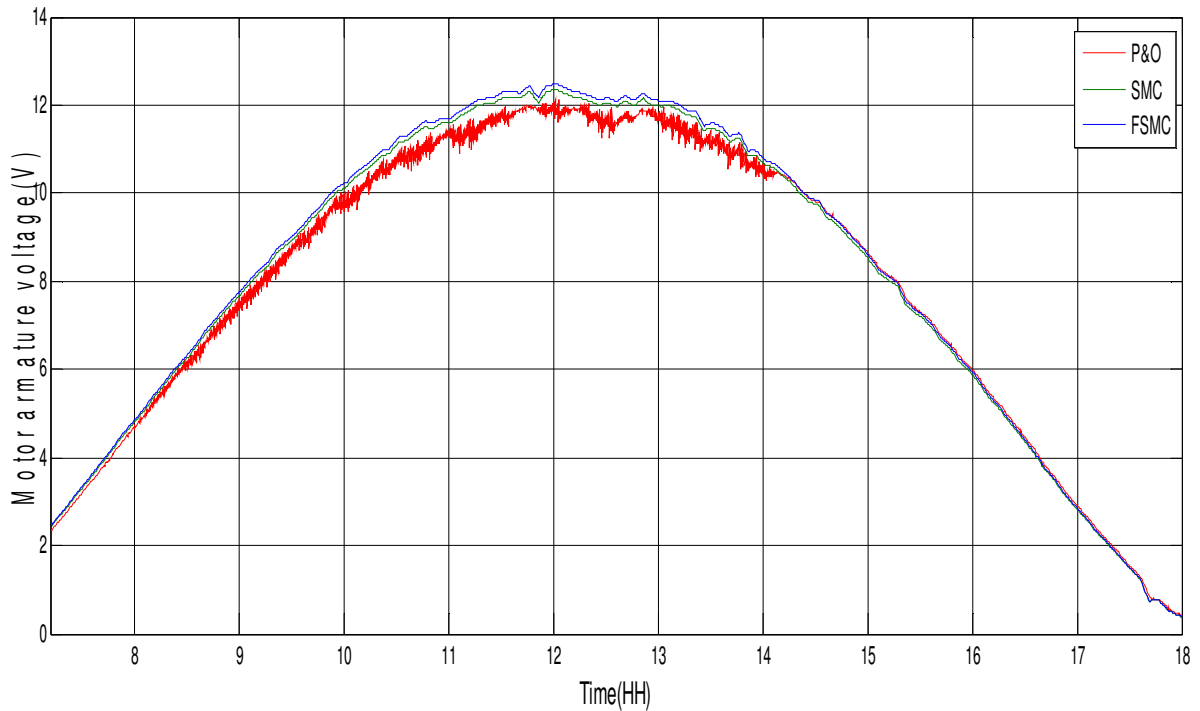


Figure 20: Motor armature voltage

We notice in figure 18 and 19 that at sunrise, there is a small delay in both methods SMC and FSMC, compared to the P&O, due to the large calculation. However, during the daytime when large quantities of water are needed the SMC and FSMC performances are much better than the P&O.

In addition, comparing the SMC to the FSMC, the curve of the later is higher than the SMC in all the figures of simulation, which proves that adding the fuzzy logic to the sliding mode limit the chattering phenomena around the sliding surface, and therefore improves the performance of the controller.

## 5. Conclusion

This paper represents a comparison between three control method: P&O, sliding mode control and fuzzy sliding mode control, which have been designed and simulated for the proposed system PV water pumping system using a DC/DC boost converter, and the test has been done for different temperature and irradiation, all the simulations were done under Matlab/Simulink.

Lot of methods to incorporate sliding mode control with fuzzy logic control exist. As known, sliding mode control consist of two parts equivalent control and stability control. in this paper, we have chosen to replace the stability part with a fuzzy logic controller.

Hence, from simulations results, it is clear that the proposed fuzzy sliding mode control gives better performance at tracking the maximum power point, with minimum oscillations regardless of the variation of meteorological parameters, therefore a higher speed for the DC motor and flow rate for the pump, and the calculation of the efficiency factor for each

proposed MPPT controller, is just another prove that the FSMC is more efficient and better tracker than Sliding Mode Controller alone or P&O algorithm.

## Reference

- [1] M. Berrera, A. Dolara, R. Faranda, and S. Leva, "Experimental test of seven widely-adopted MPPT algorithm," IEEE Bucharest Power Tech Conference 2009, pp. 1 - 8.
- [2] Dolara, R. Faranda, S. Leva, "Energy Comparison of Seven MPPT Techniques for PV Systems", Journal of Electromagnetic Analysis and Applications, vol.1, no.3, pp.152-162, Sep 2009.
- [3] J.H.Su, J.J.Chen, and D.S.Wu, "Learning feedback controller design of switching converters via MATLAB/SIMULINK," IEEE Trans. Educ., vol. 45, no. 4, pp. 307-315, Nov. 2002.
- [4] H. Tian, F. Mancilla-David, K. Ellis, E. Muljadi, P Jenkins, A cell-to-module-to-array detailed model for photovoltaic panels, Solar Energy Volume 86, Issue 9, September 2012, Pages 2695–2706.
- [5] G. Anandhakumar, M. Venkateshkumar, P. Shankar, Fuzzy Logic Controller Based MPPT Method of the Photovoltaic Power System, International Review of Automatic Control, Vol 7, No 3, 2014.
- [6] M. Benghanem, Performances of photovoltaic water pumping systems: a case study, International Journal of Renewable Energy Technology 2009 - Vol. 1, No.2 pp. 155 - 172.
- [7] A. Hadji Arab, M. Benghanem, and F. Chenlo, Motor-Pump system modelization, Renewable Energy, vol. 31, pp. 905913, 2006.
- [8] M. A. Elgendy, B. Zahawi, and D. J. Atkinson, Analysis of the performance of DC photovoltaic jumpings systems with maximum power point tracking, in Proc. IET Int. Conf. Power Electronics, Machines and Drives, York, U.K., 2008, pp. 426430.
- [9] M. Akbaba, Optimum matching parameters of an MPPT unit based for a PVG-powered water pumping system for maximum power transfer, Int. J. Energy Res., vol. 30, pp. 395409, 2006.
- [10] İ. Mustafa, D. Tugçe, T. Mehmet, Fuzzy Logic Controlled DC-DC Converter Based Dynamic Voltage Restorer, Journal of Electrical Systems . 2015, Vol. 11 Issue 4, p367-675. 9p.
- [11] Y. Weslati, A. Sallemi, F. Bacha, and R. Andoulsi, "Sliding mode control of a photovoltaic grid connected system," Journal of Electrical Systems ISSN 1112-5209, vol. 4, issue 3, September 2008.
- [12] Slotine JE and Li W (2005) Applied nonlinear control, 3rd ed. Reading, MA: Addison Wesley.
- [13] Walker, Geoff1, "Evaluating MPPT Converter Topologies Using a Matlab PV Model" Journal of Electrical & Electronics Engineering, Australia Volume 21 Issue 1 (2001).
- [14] V. I. Utkin, "Sliding mode control design principles and applications to electric drives" IEEE Transactions on Industrial Electronics (Volume:40 , Issue: 1 )
- [15] K. David, Vadim I. Utkin, "A Control Engineer's Guide to Sliding Mode Control" IEEE Transactions on Control Systems Technology, VOL. 7, NO. 3, MAY 1999.
- [16] A. H. ALQahtani, V. I. Utkin, "Control of Photovoltaic System Power Generation Using Sliding Mode Control" Power System Technology (POWERCON), 2012 IEEE International Conference.
- [17] Chen-ChiChu ,Chieh-LiChen, "Robust maximum power point tracking method for photovoltaic cells: A sliding mode control approach", SolarEnergy Vol. 83, 2009, pp. 1370-1378.
- [18] Mahmoud Ellouze, Riadh Gamoudi and Abdelkader Mami, Sliding mode control applied to a photovoltaic water- pumping system, International Journal of Physical Sciences Vol. 5(4), pp. 334-344, April 2010.
- [19] J. Ghazanfari and M. Farsangi, "Maximum power point tracking using sliding mode control for photovoltaic array," Iranian Journal of Electrical & Electronic Engineering, vol. 9, no. 3, p. 189, 2013.
- [20] M. A. Elgendy, B. Zahawi and D. J. Atkinson, Assessment of Perturb and Observe MPPT algorithm implementation techniques for PV pumping applications, IEEE transactions on sustainable energy, pp.21-33, Vol 3, No 1, 2012.
- [21] CHUEN CHIEN LEE "Fuzzy Logic in Control Systems: Fuzzy Logic Controller-Part I" IEEE Transaction on systems, man, and cybernetics, vol. 20, no. 2, March/April 1990.